The Stellar Content of the Polar Rings in the Galaxies NGC 2685 and NGC 4650A[1]

G.M. Karataeva[1], I.O. Drozdovsky[2], V.A. Hagen-Thorn[1] and V.A. Yakovleva[1]

Astronomical Institute, St.Petersburg State University, Universitetskii pr., 28, Petrodvoretz, St.Petersburg, 198504, Russia

N.A. Tikhonov[3] and O.A. Galazutdinova[3]

Special Astrophysical Observatory, N.Arkhyz, Karachai-Circassian Rep., 369167, Russia

ABSTRACT

We present the results of stellar photometry of polar-ring galaxies NGC 2685 and NGC 4650A, using the archival data obtained with the Hubble Space Telescope's Wide Field Planetary Camera 2. Polar rings of these galaxies were resolved into ~ 800 and ~ 430 stellar objects in the B, V and I_c bands, considerable part of which are blue supergiants located in the young stellar complexes. The stellar features in the CM-diagrams are best represented by isochrones with metallicity Z = 0.008. The process of star formation in the polar rings of both galaxies was continuous and the age of the youngest detected stars is about 9 Myr for NGC 2685 and 6.5 Myr for NGC 4650A.

Subject headings: galaxies: individual: (NGC 2685, NGC4650A) — galaxies: peculiar — galaxies: starburst — galaxies: stellar content

---

[1]Isaac Newton Institute of Chile, St.Petersburg Branch

[2]Visiting Astronomer, SIRTF Science Center, California Institute of Technology, MS 220-6 Pasadena, CA 91125, USA

[3]Isaac Newton Institute of Chile, SAO Branch

[1]Based on observations made with the NASA/ESO Hubble Space Telescope, obtained from the Space Telescope Science Institute, which is operated by the Association of Universities for Research in Astronomy, Inc., under NASA contract NAS5-26555.

1. Introduction

Polar-ring galaxies (PRGs) represent a rare class of peculiar objects containing a ring or annulus of gas, stars and dust orbiting in a plane nearly perpendicular to the equatorial plane of the host galaxy. This unique geometry of PRGs gives an ideal opportunity to investigate the shape of their 3D gravitational potential. Typically, the host galaxy looks like a galaxy of early morphological type but with some peculiarities in color and brightness distribution; sometimes these properties let this component more similar to a late-type object rather than to an S0 galaxy (e.g. Arnaboldi et al. 1995; Iodice et al. 2002). Recently polar rings (PRs) have also been found around spiral galaxies NGC 660 (van Driel et al. 1995) and UGC 5600 (Karataeva et al. 2001). The main properties of polar rings (compiled by Bournaud & Combes (2003)) are similar to those of spiral arms: blue color, plenty of gas and dust, prominent star forming regions, and disk-like rotation.

According to the most popular point of view, PRGs are the result of galaxy interaction, ranging from simple gas accretion (e.g. Schweizer et al. 1983) to complete merger (Bekki 1997). Both hypotheses are investigated in detail by Bournaud & Combes (2003). The authors conclude that both scenarios may explain the PRGs formation but the accretion one is preferable because some predictions relative to the merging scenario (such as the stellar halo around the polar ring) are not observed. Alternatively, polar rings can represent the delayed inflows of primordial gas (e.g. Toomre 1977; Curir & Diaferio 1994).

Intensive studies of this strange objects have been started after publication of the atlas and catalogue of PRGs and candidates for these objects (Whitmore et al. 1990), though strong emission lines in the spectra of PRs were detected before (e.g. Schechter & Gunn 1978; Schweizer et al. 1983). The presence of HII-regions in the PRs of some nearby galaxies, such as NGC 2685 (Makarov et al. 1989; Eskridge & Pogge 1997) and NGC 4650A (Eskridge & Pogge 1999), the optical colors and Hα luminosities of the rings (Reshetnikov & Combes 1994) as well as high IR-fluxes of PRGs (Richter et al. 1994) suggest a presence of active star formation in PRs.

We present here a deep optical study based on *HST* WFPC2 archival data of the resolved stellar populations of two nearby PRGs, NGC 2685 (D$\sim$ 12.5 Mpc), and NGC 4650A (D$\sim$ 35 Mpc) (H_0 =75 km/s/Mpc). Multi-color stellar photometry provides the opportunity to study directly the resolved stellar populations of different masses, ages and chemical abundances. The analysis of the stellar distribution on Color-Magnitude Diagrams (CMDs) is the most powerful way to investigate population fractions and their spatial variations, to estimate the galaxy distance, and to provide clues to its star formation history (e.g. Tolstoy 1999).

Both galaxies were included by Whitmore et al. (1990) in the group of most probable PRGs, 'A', having two well-established orthogonal kinematic systems on the basis of optical (Sersic & Aguero 1972; Schechter & Gunn 1978; Schechter et al. 1984) and radio-HI observations (Shane 1980). The important difference between these galaxies is that the polar ring of NGC 2685 is comparable in size to the host galaxy, while NGC 4650A has a polar ring extended out to more than two radii of the host galaxy.

NGC 2685 (Arp 336, also known as "The Helix galaxy" and "The Spindle") has long been known as an unusual object (Sandage 1961). Fig. 1 presents its image taken from the The Digitized Sky Survey. Sandage (1961) pointed to the singularity of NGC 2685, and later Arp (1966) included the galaxy in his atlas of peculiar galaxies. The main body of the galaxy having a spindle-like shape is twisted by luminous filaments (rings) traced by dark strips on the central galaxy. Deep images (see Sandage (1961)) reveal an outer extended low luminosity elliptical structure (outer ring) with position angle close to that of the galaxy major axis. The combination of photometric (Hagen-Thorn et al. 1983; Makarov et al. 1989) and spectroscopic (Schechter & Gunn 1978) data shows that NGC 2685 is most likely an edge-on S0 galaxy with rings (helices) rotating approximately perpendicular to the main optical disk. The HI map (Shane 1980; Schinnerer & Scoville 2002) also shows an extended structure coincided with outer ring. One small, 16th magnitude galaxy lies within $10'$(36 kpc in projection) of NGC 2685 and two more faint, small galaxies are within $20'$(Richter et al. 1994). If they are not background objects,then the gas capture during the galactic interaction might produce such a peculiar morphology.

Galaxy NGC 4650A (Fig. 2) is a prototype of PRGs with extraordinary extended polar ring (Sersic 1967). Its structure was investigated in detail in many works (e.g. Gallagher et al. 2002; Iodice et al. 2002). As in the case of NGC 2685 the central galaxy of NGC 4650A looks like an edge-on S0 galaxy but just this galaxy has peculiar brightness distribution and colors. The ring, which is about $2-3$ times the size of the central disk, is inclined with $\sim 100^\circ$ angle to the galaxy's major axis. The dark strip of absorption is visible at the place where ring is projected on the central galaxy. The ring itself has a complex structure: in the central part it is inclined to the line of sight and both parts are visible; howere, at the distance of $30''$, they supposedly overlap when the ring become seen as edge-on. Some of separate filaments are visible in the outer regions of the ring. According to Arnaboldi et al. (1997) the ring demonstrates some signs of spiral structure.

Data available in the literature concerning the color of NGC 2685 polar ring are inconsistent. In (Hagen-Thorn et al. 1983; Makarov et al. 1989) it has been shown on the basis of UBV surface photometry that a color of the ring is typical for the spiral arms of $Sb-Sc$ galaxies. Peletier & Christodoulou (1993) found later that rings color is close to that of cen-

tral galaxy, i.e. is red. However, this result is unclear due to uncertainty of transformation of their J and F mag to the standard Johnson BV magnitude photometric system without taking into account the large radiation contribution of the emission lines.

The color of NGC 4650A polar ring is blue: $B-V \sim -0\overset{\mathrm{m}}{.}1$, according to Schechter et al. (1984) or $B-V \sim 0\overset{\mathrm{m}}{.}2 \div 0\overset{\mathrm{m}}{.}3$, according to Iodice et al. (2002).

Both galaxies were observed in the CO line $J = 2-1$ (Watson et al. 1994; Schinnerer & Scoville 2002). It is established that the emission is associated solely with the polar rings. Watson et al. (1994) claimed that in NGC 4650A the mass of H_2 was of $17\% - 35\%$ of the HI mass, while in NGC 2685 this value exceeded HI mass. But Schinnerer & Scoville (2002) have found that Watson et al. (1994) overestimated the H_2 mass in NGC 2685 by an order of magnitude. Nevertheless, both galaxies have sufficient molecular clouds for star forming activity.

There are some papers containing the claims on stellar populations and therefore the ages of polar rings (Peletier & Christodoulou 1993; Iodice et al. 2002; Gallagher et al. 2002). For all the cases, results of surface photometry were used. In Peletier & Christodoulou (1993) the age of the NGC 2685 ring was estimated as $\sim$ 5-6 Gyr on the basis of its color (however, these data are uncertain, see above). As for NGC 4650A the data on ring colors show that the young stellar population certainly exist. The detailed surface colorimetry of the galaxy was done by Iodice et al. (2002) and Gallagher et al. (2002). In the first paper the ages of 1-3 Gyr for the central region of the host galaxy and $< 10^8$ yr for polar ring were found, while Gallagher et al. (2002) claimed that the ages of the host galaxy and the ring are 3-5 Gyr and $\sim$ 1 Gyr, correspondingly.

A study of different stellar populations of the polar rings, using their CMDs, will cast light on the origin and evolution of PRGs. We made here the first attempt to investigate the stellar population of polar rings in NGC 2685 and NGC 4650A in such a way.

2. Observations and Basic Data Processing

We make use of archival HST/WFPC2 data of NGC 2685 and NGC 4650A. The observations of NGC 2685 were carried out as part of proposal N 6633 by Marcella Carollo in January 1999. The data set consists of images in $F450W$, $F555W$,$F814W$-bands with total exposure times of 2300 sec, 1000 sec and 730 sec, accordingly. The NGC 4650A data set is based on the 7500 sec exposures in the $F450W$-band, 4763 sec in the $F606W$ and 7600 sec in the $F814W$, which were gathered under proposal N 8399 y Keith Noll in April 1999.

Figure 2 presents $F450W$ and $F814W$-band images of NGC 4650A. The blue color of the ring is evident. While WF3&4 chips of WFPC2 cover the most part of NGC 4650A polar ring, the south part of NGC 2685 and its ring are missing in the WFPC2 data. Total size of the NGC 2685 according to RC3 is $4\farcm5 \times 2\farcm3$. At the distance of NGC2685 $1''$ corresponds to about 60 pc. For NGC4650A $1''$ corresponds to about 170 pc.

The raw frames were processed with the standard WFPC2 pipeline. The data were extracted from the Archive using the on-the-fly reprocessing STScI archive system, which reconstructs and calibrates original data with the latest calibration files, software, and data parameters. When it was possible we used the recent version of the `DitherII` package, which performs a "drizzling" (a variable-pixel linear for correcting reconstruction) and corrects for geometric distortion. The processed frames were then separated into images for each individual CCD, and trimmed of the vignetted regions using the boundaries recommended in the WFPC2 Handbook. The images were combined after cleaning them for bad pixels and cosmic-ray events.

The single-star photometry of the images was processed with `DAOPHOT/ALLSTAR`. To avoid contamination by galactic background emission single-star photometry was performed on images with subtracted median-smoothed (with a window of $10 \times (FWHM)$) shape. The PSF was modeled and evaluated for each chip. The search of the stellar objects was made using the master frame produced from all images. The resulting list of stellar coordinates was given to `ALLSTAR` to perform the photometry in the individual frames. The necessary corrections were applied to resulting photometric data including a correction for Charge-Transfer Inefficiency. Transformation of Holtzman et al. (1995) was used to convert instrumental magnitudes to the standard $B(F450W)$, $V(F555W, F606W)$, and $I_{\rm c}(F814W)$ system.

$F606W$-band is a wide 'Hα continuum' and includes Hα. It may influence on the accuracy of the NGC 4650A V-band photometry. Different band star lists were merged requiring a positional source coincidence better than $0.5 \times FWHM$, or a box size of 2 pixels.

Completeness test was performed using the usual procedure of artificial star trials (Stetson 1994). A total of 1,500 artificial stars were added to the $F450W$,$F606W$ ($F555W$) and $F814W$-band frames in several steps of 150 stars each. These had magnitudes and colors in the range $18\fm0 \leq I_{\rm c} \leq 28\fm0$ and $0\fm5 \leq (V - I_{\rm c}) \leq 1\fm5$. Stars were considered as recovered if they were found in all the bands with magnitudes not exceeding $0\fm75$ brighter than the initial, injected ones. The results of the test are shown in Fig. 3. As one can see in NGC 2685 the recovery is practically complete up to m = $24\fm8$ in B-band , m = $24\fm6$ in V-band and m = $23\fm5$ in $I_{\rm c}$-band; for NGC 4650A up to m = $25\fm6$ in B-band, m = $25\fm2$ in V-band and m = $25\fm2$ in $I_{\rm c}$-band. For more faint objects (within $1\fm0 - 1\fm5$) the recovering fraction is

half as much.

3. Results

There are $\sim$ 450 stellar objects in NGC 4650A and $\sim$ 800 in NGC 2685 detected in B, V and I_c filters with quality parameters $SHARP$ and CHI (as defined in `ALLSTAR` in `MIDAS`) in the intervals $-1 \leq SHARP \leq 1$ and $CHI \leq 2$. Our final lists of stellar objects include objects having angular sizes $FWHM < 0\farcs15$ for NGC 4650A and $FWHM < 0\farcs40$ for NGC 2685. Figure 4 illustrates the precision of our photometry.

The magnitudes and colors of these objects were corrected for extinction in our galaxy using IRAS/DIRBE map of Schlegel et al. (1998). With $R_V = 3.1$ and the extinction law of Cardelli et al. (1989), galactic foreground extinction for NGC 4650A is: $A_B = 0\fm48$, $A_V = 0\fm37$, and $A_{I_c} = 0\fm22$; and for NGC 2685: $A_B = 0\fm27$, $A_V = 0\fm21$, and $A_{I_c} = 0\fm12$. The extinction-corrected data are used for construction of color- magnitude and color-color diagrams. CMDs (B vs $(B - I_c)$) for NGC 2685 and NGC 4650A are given in Figure 5.

Among detected point objects the bulk of which are evidently blue giants and supergiants the outside objects with dimensions less than 25 pc may be present. The possible candidates are unresolved double and multiple stars, super star clusters (SSC) with typical dimensions of $8 \div 10$ pc, compact HII-regions, and more extended HII-regions with typical dimensions of about 20 pc.

It is difficult to separate multiple stars from single supergiants in our data, but a portion of systems in which single blue supergiant is not dominant probably is not high (see below). There are no SSCs among our objects. Having mean absolute magnitudes of $M_V = -13^m$ (Whitmore et al. 1993) SSCs at the distance of NGC 2685 (m-M = $30\fm5$) will have an apparent magnitude of $17\fm5$ and $19\fm7$ at the distance of NGC 4650A (m-M = $32\fm7$). There are no such bright objects among those listed. HII-regions can be separated using two-color diagrams. Since the Hα emission penetrates to the $F606W$-band the $V - I_c$ color for HII-regions proves to be less than one for blue stars ($V - I_c \sim -0\fm35$). Therefore, HII-regions have bluer color in $V - I_c$ than in $B - I_c$. As a result all questionable objects were excluded from the final lists, which contain 430 stars for NGC 4650A and 800 stars for NGC 2685.

3.1. NGC2685

In Fig. 6,(*left*) the location of blue (circles) and red (squares) supergiants of NGC 2685 is shown. It is evident that most part of both are concentrated to the region of polar rings

(though some objects in the lower-right corner, perhaps, belong to the outer ring).

In the Fig. 6,(*right*) we give in enlarged scale the map of the portion of galaxy near polar ring in which circles are the most blue regions found after dividing frame $F814W$ by $F550W$. All of these coincide with HII-regions. From comparison Fig. 6, (*left*) and Fig. 6, (*right*) the correlation between locations of HII-regions and blue supergiants is evident.

As one can see in the Fig. 6, the amount of red supergiants is quite small. It is noticeable that both red and blue supergiants tend to gather into stellar associations. This fact also confirms that the detected stars are red supergiants of the polar ring rather than foreground Galactic red stars.

In the color-magnitude diagram B vs $(B - I_c)$ (Fig. 5) the blue limit of the stars is shifted to the red in comparison with normal position for blue supergiants which can be found from (Bertelli et al. 1994). This fact point to significant intrinsic absorption in polar rings.

Comparison of the blue limit of the stars for the galaxy with that found for galaxies without intrinsic absorption gives the color-excess for the galaxy. But blue limit at CMDs is not sharp because of different absorption for various stars and their different ages and metallicity. Therefore it is more reliable to use as a compared parameter the color-index for which the maximum in number of blue stars is observed (this value gives the mean color index for blue supergiants and may be found after constructing the corresponding histogram).

For NGC 2685 $(B - I_c)^{max} = +0\overset{m}{.}25$; the comparison with galaxies NGC 959 ($(B - I_c)^{max} = -0\overset{m}{.}18$) and HolmII ($(B - I_c)^{max} = -0\overset{m}{.}10$) (our unpublished data; both galaxies may be considered as galaxies with negligible intrinsic absorption) gives $E_{(B-I_c)} = 0\overset{m}{.}39$.

There is direct determination of absorption in the rings obtained from the surface photometry (Hagen-Thorn et al. 1983). It is known that the north-east part of the main body of the galaxy is intersected by four dark strips for which in the absorption was found (Hagen-Thorn et al. 1983). These strips are the result of projection on the main body of polar rings which are luminous outside the galaxy (they simply follows each other). For normal extinction curve (Cardelli et al. 1989) and mean value of absorption in B-band for all four strips one can find $E_{(B-I_c)} = 0\overset{m}{.}35$.

The total absorption in several HII-regions was obtained by Eskridge & Pogge (1997) on the basis of Balmer decrement. The authors found that absorption A_V is essentially different in different HII-regions (from $0\overset{m}{.}00$ to $0\overset{m}{.}77$). After correction for galactic extinction it gives $E_{(B-I_c)} = 0\overset{m}{.}40$ for the most obscured HII-regions.

Two latter estimations do not contradict to the value $E_{(B-I_c)} = 0\overset{m}{.}39$ found above.

Therefore we accept this. Since there is no possibility to correct for intrinsic absorption the data for individual stars we take it into account *in average*, reducing for all stars the color index $B - I_c$ by $0\overset{m}{.}39$ and magnitudes B, V and I_c by $0\overset{m}{.}74, 0\overset{m}{.}56, 0\overset{m}{.}35$, accordingly.

The resulting M_{I_c} vs $B - I_c$ diagram (for m-M = $30\overset{m}{.}5$) is shown in Fig. 7, *left*.

3.2. NGC4650A

In the CMD for NGC 4650A (Fig. 5) crosses are unresolved HII-regions selected using two-color diagram. They have been excluded from the final list.

The location of detected blue stars in the field of NGC 4650A is shown in Fig. 8, *left*. The blue objects are evidently concentrated to the polar ring. Note that some stars follows so called "spiral arms" (Arnaboldi et al. 1997; Gallagher et al. 2002) especially in their south branch. As one can see in Fig. 8, *right* red stars are distributed randomly without any concentration to the galaxy and are, therefore, foreground stars belonging to our Galaxy. (In NGC 4650A we cannot reach the red giants which might consist a halo around polar ring as the merging scenario demands.)

A comparison of the distribution of blue objects with the Hα image of the galaxy (Eskridge & Pogge 1999) shows (as in the case of the NGC 2685) a correlation between location HII-regions and blue stars.

It is difficult to correct for intrinsic absorption in this case. According to Gallagher et al. (2002) there is a dust ring in the center of the galaxy. Iodice et al. (2002) give the $A_B = 1\overset{m}{.}54$, $A_{I_c} = 1\overset{m}{.}00$ for the extinction in the place of the ring projection on the main body. These values may be considered as an upper limit of intrinsic absorption in the ring outside the main body in regions of dust ring. But extreme blue ring colors far off the galactic center show that the extinction is very small (if any) in these regions. We attempt to introduce the correction for intrinsic absorption as linear along the polar ring from the center to periphery but without success because the scatter in the CMD along $B - I_c$ axis has not decrease. Therefore, we did not apply any correction for intrinsic absorption keeping in mind that in reality stars at CMD may be located more left.

The resulting M_{I_c} vs $B - I_c$ diagram (for m-M = $32\overset{m}{.}7$) is shown in Fig. 7, *right* .

4. Discussion

The important argument that benefits the assumption that most of the objects are blue supergiants gives the construction of luminosity functions (LFs) for blue objects in both galaxies. Luminosity function was calculated for all objects with $B - I_c < 0\overset{m}{.}8$ for NGC 4650A and $B - I_c < 1\overset{m}{.}2$ for NGC 2685 (taking into account its reddening of $E_{(B-I_c)} = 0\overset{m}{.}39$) by counting stars lying inside a bin of $0\overset{m}{.}5$. The central value was varied in steps of $0\overset{m}{.}25$ to reduce the dependence of our results on the particular choice of bin center. The results are given in Fig. 9.

As it was shown by Freedman (1985) the slope of the luminosity function for blue supergiants is similar for all spiral galaxies with mean value of about 0.6. The slope of luminosity function in the bright part (where the completeness is close to 100%) is 0.62 ± 0.01 for NGC 4650A and 0.61 ± 0.02 for NGC 2685 (dashed lines in Fig. 9), being in agreement with Freedman (1985) value. Thus the results show that the polar rings contain young blue supergiants testifying that stars-forming processes are still going there.

The "color-absolute magnitude" diagrams for both galaxies presented in Fig. 7 demonstrate mostly the brightest and youngest stellar populations. CMD for NGC 2685 is deeper in comparison with that of NGC 4650A but still does not reach an area of old/intermediate-age stellar populations, for example, red giants ($M_{I_c} \approx -4\overset{m}{.}0$). The discovery of red giants (old population) would allow to estimate the age of the rings.

In Fig. 7 the theoretical stellar isochrones from Bertelli et al. (1994) are overplotted for the metallicity of Z = 0.008 and ages from 7 to 33 Myr. Such a metallicity is usual for irregular galaxies (Garnett 2002). Isochrones for this metallicity are in good agreement with CMDs observed by us. We do not find any confirmation of high metallicity in NGC 2685 found by Eskridge & Pogge (1997) who used empirical method of its determination, which strongly depends on accepted intrinsic absorption for HII regions. The isochrones for higher metallicity (e.g. solar) certainly contradict with CMD observed.

From Fig. 7 we can infer that process of star formation was continuous during tens of Myrs, and the last burst of star formation probably was more recent in NGC 4650A than in NGC 2685.

5. Conclusions

The main result of this work is resolution of the stars in the PRs of NGC 2685 and NGC 4650A. B, V, I_c photometry was made for several hundreds of stars (mostly blue giants

and supergiants) in each galaxy. Our research is the first one relating to resolvable stellar population in polar rings.

The distribution of blue and red supergiants in the field of galaxies strongly follows the polar rings. The stars tend to gather into stellar associations which positions are correlated with positions of HII regions.

CMDs for both galaxies show that process of star formation is continuous during tens Myrs, the last burst of star formation being very recently (6.5 Myr in NGC 4650A and 9 Myr in NGC 2685). Unfortunately, CMDs for both galaxies are insufficiently deep to claim anything about the old population in the rings. But for NGC 2685 the upper limit of red giants branch may be reached with more deep exposures at HST and planning such observations is very desirable. These observations might also verify whether a stellar halo exist around the main galaxy as predicted by (Bournaud & Combes 2003) for merging scenario of PRGs formation.

This work was supported by RFBR via grants 03-02-16344 and 02-02-16033.

REFERENCES

Arnaboldi M., Freeman K.C., Sackett P.D., Sparke L.S., capaccioli M. 1995, Planet Space Sci., 43, 1377

Arnaboldi M., Oosterloo T., Combes F., Freeman K.C., Koribalski B. 1997, AJ, 113, 585

Arp H.C. 1966, Atlas of Peculiar Galaxies (California Institute of Technology, Pasadena)

Bekki K. 1997, ApJ, 490, L37

Bertelli G., Bressan A., Choisi C., Fagotto F., Nasi E. 1994, A&AS, 106, 275

Bournaud F., Combes F. 2003, A&A, 401, 817

Cardelli J.A, Clayton G.C., Mathis J.S. 1989, ApJ, 345, 245

Curir A., Diaferio A. 1994, A&A, 285, 389

Eskridge P.B., Pogge R.W. 1997, ApJ, 486, 259

Eskridge P.B., Pogge R.W. 1999,in ASP Conf.Ser. 163, Star Formation in Early-Type Galaxies, ed. P.Carral & J.Cepa (San Francisco:ASP), 197

Freedman W.L. 1985, ApJ, 299, 74

Gallagher J.S., Sparke L.S., Matthews L.D., English J., Kinney A.L., Iodice E. & Arnaboldi M. 2002, ApJ, 568, 199

Garnett D. 2002, ApJ, 581, 1019

Hagen-Torn V.A., Popov I.I., Yakovleva V.A. 1983, Afz, 19, 325

Holtzman J.A., Burrows C.J., Casertano S., Hester J.J., Trauger J.T., Watson A.M., & Worthey G., 1995, PASP, 107, 1065

Iodice E., Arnaboldi M., De Lucia G., Gallagher J.S., Sparke L.S., Freeman K.C. 2002, AJ, 123, 195

Karataeva G.M., Yakovleva V.A., Hagen-Thorn V.A. & Mikolaichuk O.V. 2001, Astron.Lett., 27, 74

Makarov V.V.,Reshetnikov V.P., Yakovleva V.A. 1989, Afz, 30, 15

Peletier R.F., Christodoulou D.M. 1993, AJ, 105, 1378

Reshetnikov V.P., Combes F. 1994, Violent Star Formation From 30 Dorades to QSOs, ed. Tenorio-Tagle (Cambridge University Press), 258

Richter O.-G., Sackett P.D., Sparke L.S. 1994, AJ, 107, 99

Sandage A.R. 1961, The Hubble Atlas of Galaxies (Washington)

Schechter P.L., Gunn J.E. 1978, AJ,83, 1360

Schechter P.L., Ulrich M.- E., Boksenberg A. 1984, ApJ, 277, 526

Schinnerer E., Scoville N. 2002, ApJ, 577, L103

Schlegel D.J., Finkbeiner D.P., Davis M. 1998, ApJ, 500, 525

Schweizer F., Whitmore B.C., Rubin V.C. 1983, AJ, 88, 909

Sersic J.L. 1967, Z.Astrophys., 67, 306

Sersic J.L., Aguero E.L. 1972, Ap&SS, 19, 387

Shane W.W. 1980, A&A, 82, 314

Stetson P.B. 1994, PASP, 106, 250

Tolstoy E. 1999, in IAU Symp.192, The Stellar Content of Local Group Galaxies, ed. P. Whitelock & R. Cannon (San Francisco: ASP), 218

Toomre A. 1977, The Evolution of Galaxies and Stellar Populations, eds. Larson R.B. and Tinsley B.M. (Yale University Observatory, New Haven), 418

van Driel W., Combes F., Casoli F., Gerin M., Nakai N., Miyaji T., Hamabe M., Sofue Y., Ichikawa T., Yoshida S., Kobayashi Y., Geng F., Minezaki T., Arimot N., Kodama T., Goudfrooij P., Mulder P.S., Wakamatsu K., Yanagisava K. 1995, AJ, 109, 942

Watson D.M., Guptill M.T., Buchhilz L.M. 1994, ApJ, 420, L21

Whitmore B.C., Lucas R.A., McElroy D.B., Steiman-Cameron T.Y.,Sackett P.D., Olling R.P. 1990, AJ, 100, 1489

Whitmore B.C., Schweizer F., Leitherer C., Borne K., Robert C. 1993, AJ, 106, 1354

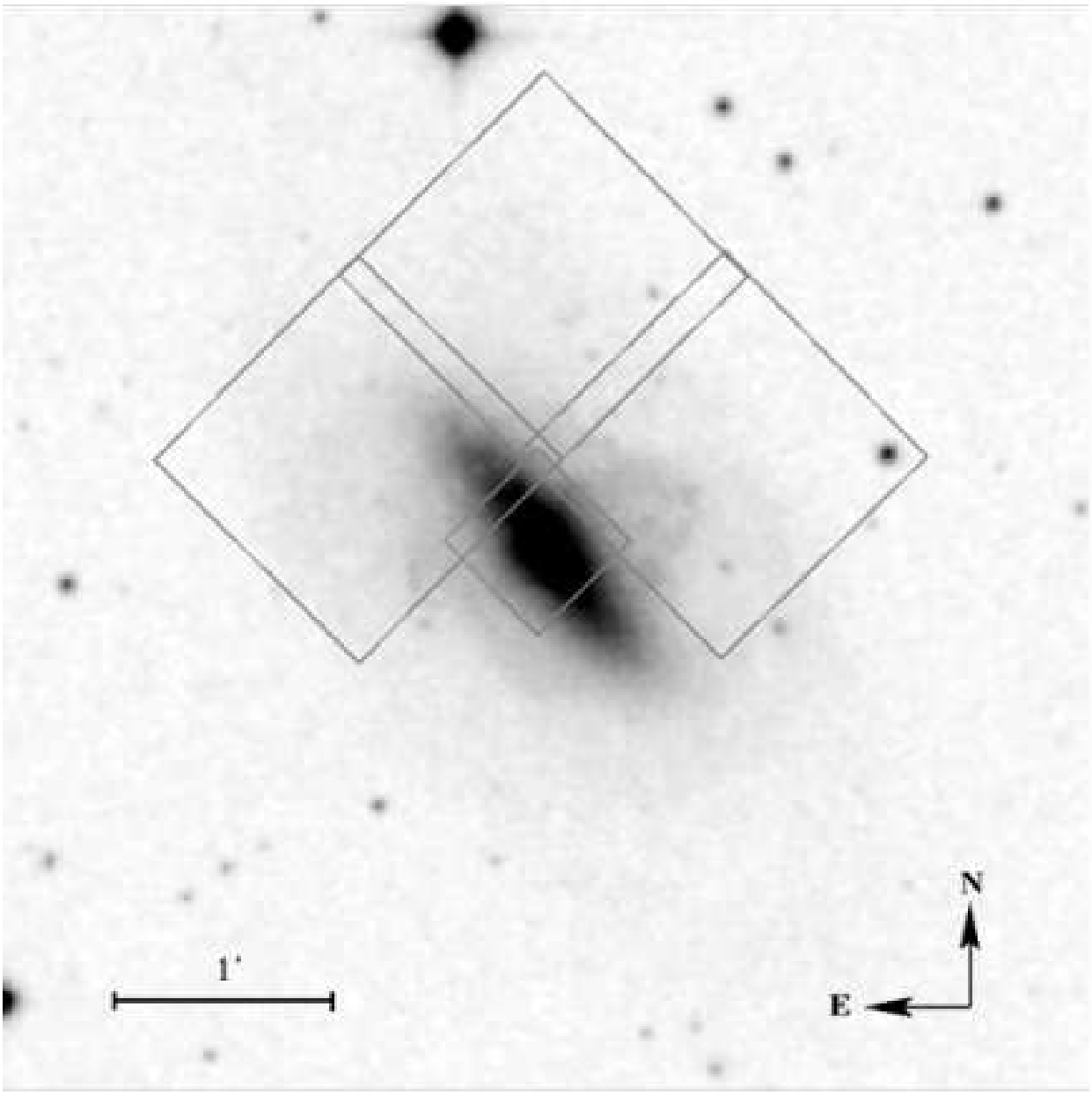

Fig. 1.— DSS $5' \times 5'$ image of NGC 2685 with WFPC2 footprint overlaid.

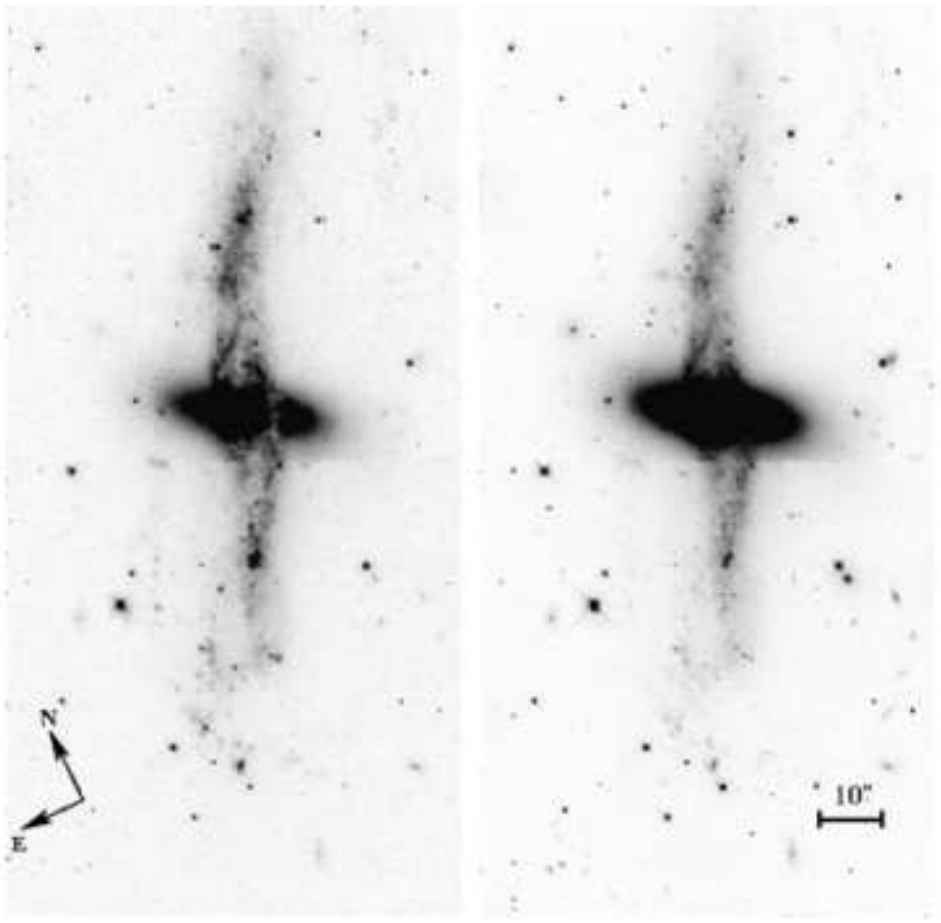

Fig. 2.— WFPC2 images of NGC 4650A (chips WF3 & 4). *Left*, the $F450W$ band image; *right*, the $F814W$ band image. The blue color of the ring is evident.

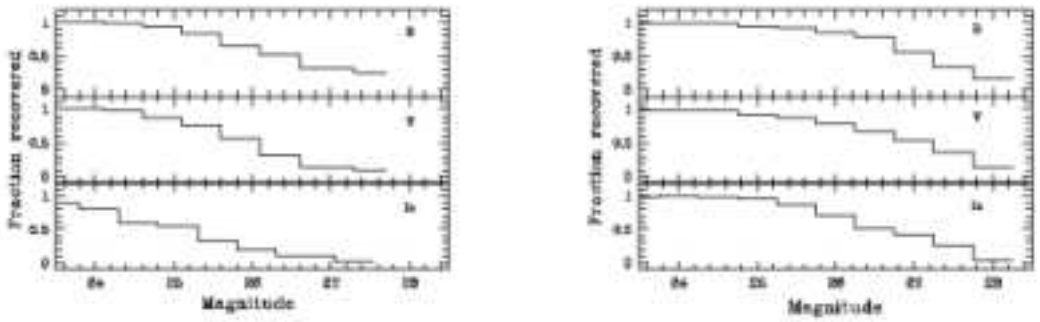

Fig. 3.— NGC 2685 (*left*) and NGC 4650A (*right*) completeness levels of the WFPC2 photometry based on artificial star tests.

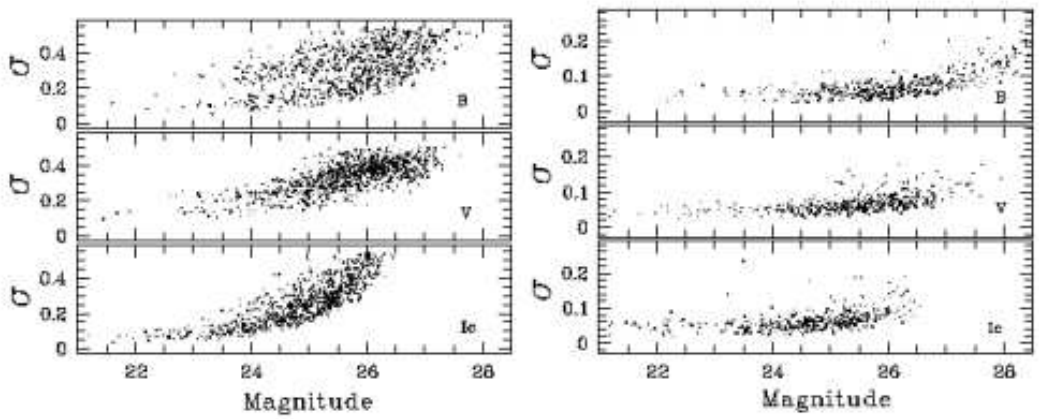

Fig. 4.— NGC 2685 (*left*) and NGC 4650A (*right*) errors of the WFPC2 photometry.

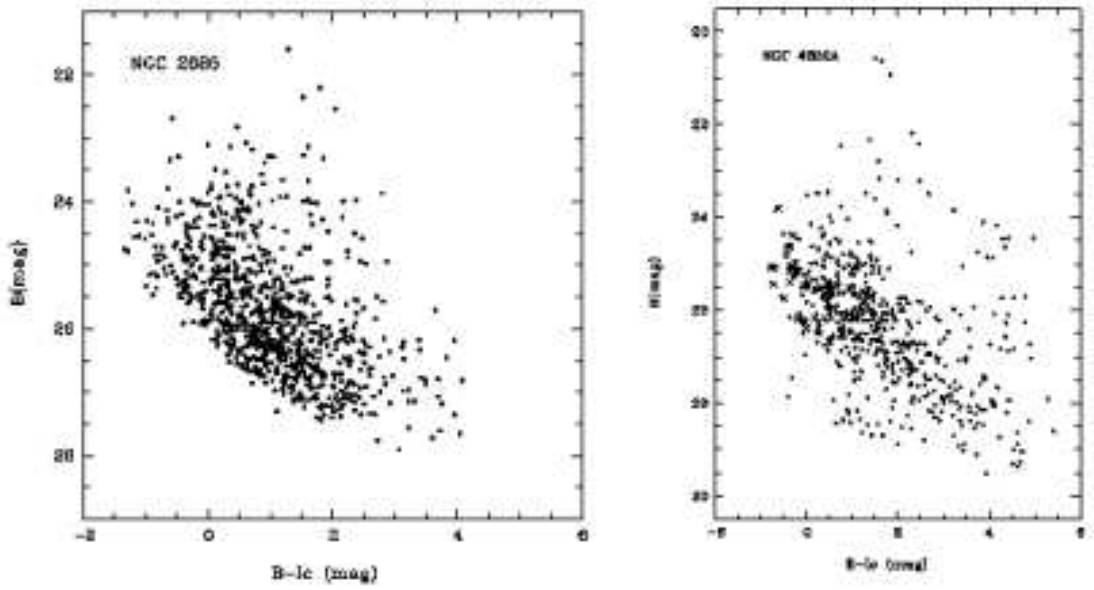

Fig. 5.— color–magnitude diagrams for NGC 2685 (*left*) and NGC 4650A (*right*) corrected for absorption in our Galaxy (crosses are unresolved HII-regions).

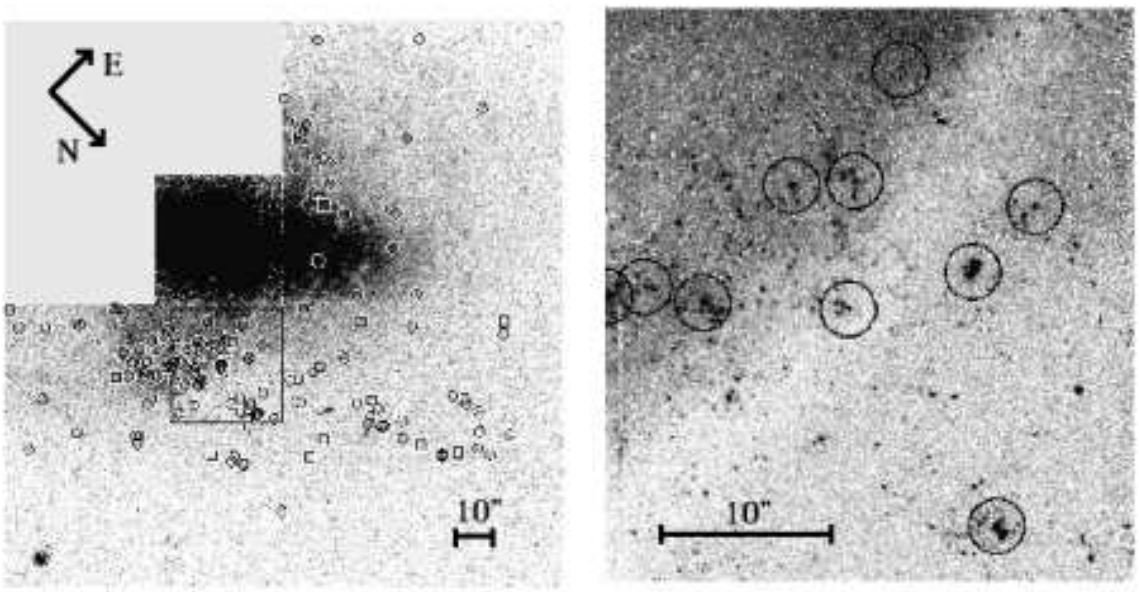

Fig. 6.— WFPC2 image of NGC 2685. Circles and squares indicate the position of blue and red supergiants, correspondingly (*left*). The candidates to HII regions in the enlarged part of NGC 2685 polar ring (*right*).

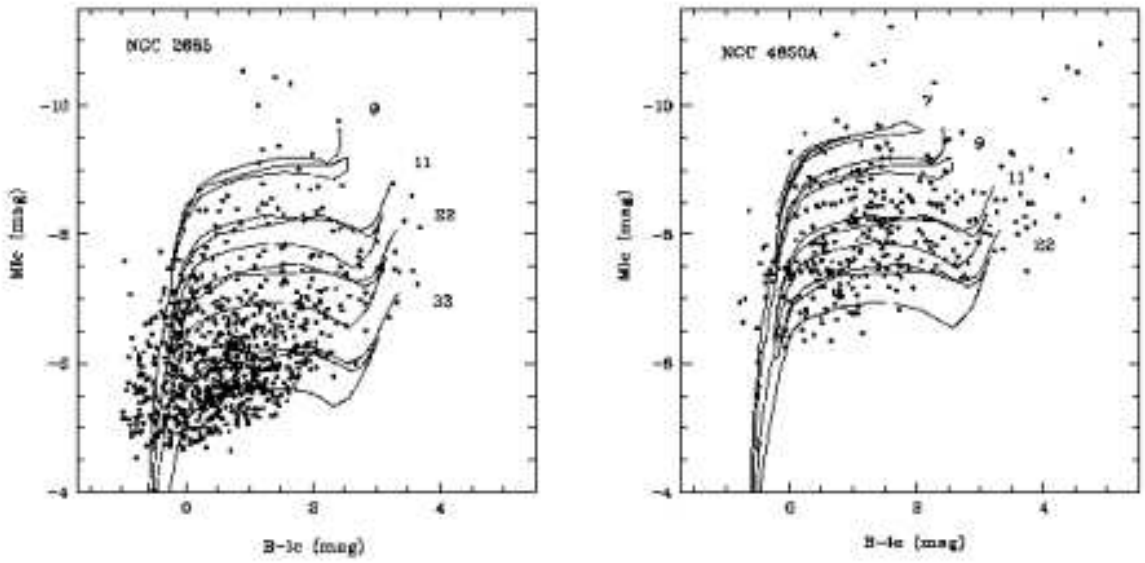

Fig. 7.— M_{I_c} vs $B-I_c$ CMDs of NGC 2685 (*left*) and NGC 4650A (*right*). Stellar isochrones for the metallicity Z=0.008 from the Padova library are overplotted for ages from 7 Myr to 33 Myr.

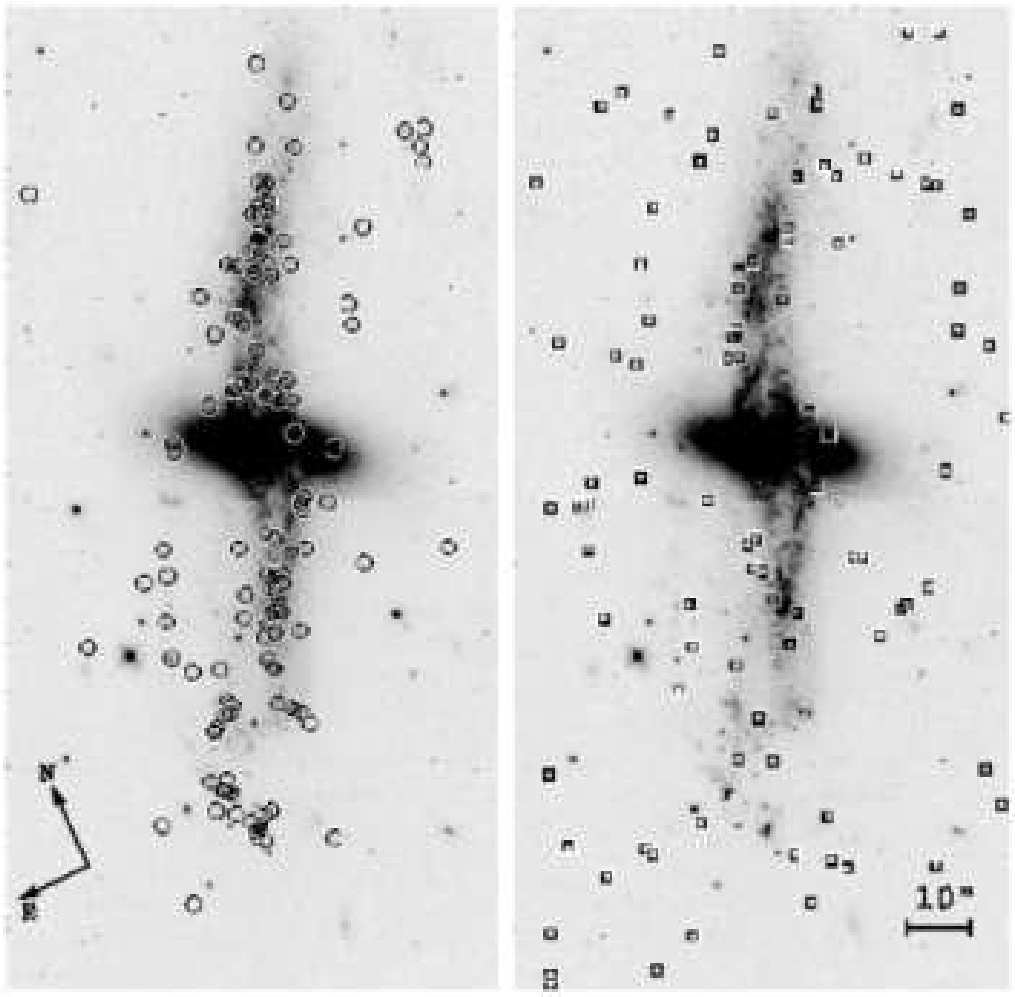

Fig. 8.— Blue supergiants (circles, *left*) in NGC 4650A and red stars (squares, *right*).

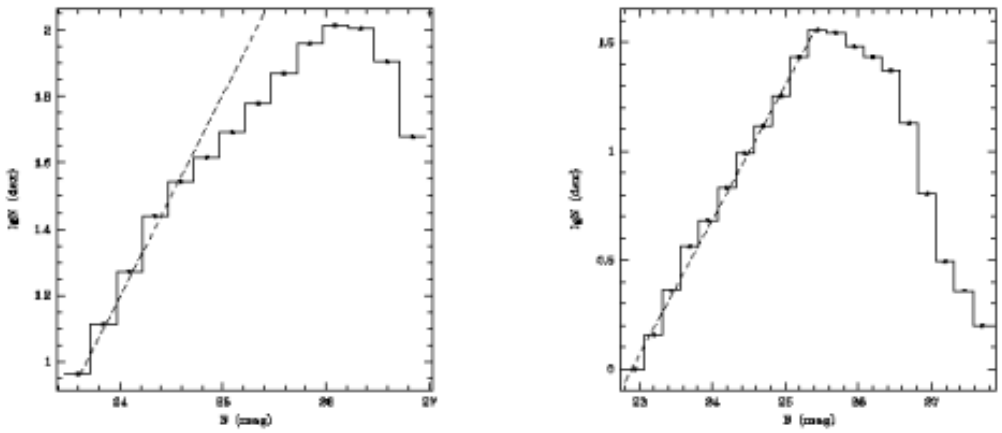

Fig. 9.— Smoothed luminosity function of blue stars (solid line) and the bright-end slope of the LF (dashed line) of NGC 2685 (left) and NGC 4650A (right).